Journal of Volcanology and Geothermal Research 201 (2011) 301–311

Contents lists available at ScienceDirect

Journal of Volcanology and Geothermal Research

journal homepage: www.elsevier.com/locate/jvolgeores

Morphometric and morphological development of Holocene cinder cones: A field and remote sensing study in the Tolbachik volcanic field, Kamchatka

Moshe Inbar [a,*], Michael Gilichinsky [b], Ivan Melekestsev [c], Dmitry Melnikov [c], Natasha Zaretskaya [d]

[a] Department of Geography and Environmental Studies, University of Haifa, Israel
[b] Department of Forest Resource Management, SLU, Umea, Sweden
[c] Institute of Volcanology and Seismology, RAS, Petropavlovsk-Kamchatsky, Russia
[d] Geological Institute, RAS, Moscow, Russia

ARTICLE INFO

Article history:
Received 14 January 2010
Accepted 18 July 2010
Available online 24 July 2010

Keywords:
Kamchatka volcanic province
Tolbachik eruption
cinder cones
morphometry
volcanic geomorphology
landscape evolution

ABSTRACT

The evolution of landscape over time is a central aspect of geological, paleogeographical and geomorphological studies. Volcanic features like cinder cones offer the opportunity to monitor the processes and development of the landscape. Cinder cones are perhaps the simplest and most common volcanic landforms in the world. Morphological and morphometric study of cinder cones has proven an efficient tool for determining their relative dates, and the erosional processes affecting them. The extensive Kamchatka volcanic province (Russian Far East), with its large Tolbachik cinder cone field, is an excellent case study for spatial and temporal classification and calibration of changes in morphometric values with time.

We show how the morphological and morphometric values of the monogenetic cinder cones, measured in the field and by digital elevation models, can be used to validate their age and erosional processes.

Field data were GPS measurements of cinder cones formed at the Tolbachik 1975–1976 eruption and of Holocene cinder cones; erosion processes on the cinder cones and lava flows were identified and evaluated. For every studied cinder cone morphometric parameters were assessed on the basis of remotely sensed data and digital elevation model. Morphometric measurements were taken of cone height and slope and average axis diameter and the height–width ratio was obtained.

The comparison of morphometric parameters calculated from ASTER DEM and topographic map clearly supports the concept of relative morphometric dating as the most recent cinder cones are always associated with the highest slopes and h/W ratio. The measured morphometric values of the recent Tolbachik cinder cones are valuable benchmark data for determining erosion rates, such as the measured values for the Paricutin cone in Mexico after the 1943 eruption. The variability of the morphometric values of the recent cinder cones is due to their lithological coarse composition. A comparison with the older cinder cones in the area shows that the climatic conditions of the Kamchatka peninsula and the slow development of vegetation cover determine a high rate of erosion and rapid change in the morphometric values, as compared to published values for other volcanic fields.

1. Introduction

Morphological studies of volcanic landforms have multiplied in recent decades, primarily after the eruption of St Helens volcano in 1980 and in the light of the need to interpret extraterrestrial morphologies (Wood, 1980a; Thouret, 1999).

Cinder cones are "perhaps the simplest and most common volcanic landforms in existence" (Wood, 1980b). It is probably the only one on the globe with a distinct and defined initial date of formation, and lasting no more than a few million years, before erosional processes flatten it, a short time in the earth's geological history. Morphological and morphometric study of cinder cones has proven an efficient tool for determining their relative dates of cinder cones and the erosional processes affecting them (Wood, 1980b; Hasenaka and Carmichael, 1985; Hooper, 1995; Inbar and Risso, 2001; Parrot, 2007). Such analyses generally attempt to measure the morphometric values of cinder cones, e.g. height, diameter, and slope, and the relations among them. The evolution of cinder cones erosion might be associated to the period of time of exposure to degradation processes. The progressive change of morphometric parameters with increasing of age is the basis for relative dating of cones by comparative measurements (Wood, 1980a; Hooper and Sheridan, 1998).

The evolution of landscape over time is a central aspect of geological, paleogeographical and geomorphological studies. Recent volcanic features like cinder cones offer the opportunity to monitor the processes and development of the landscape. Morphometric and

* Corresponding author.
E-mail address: inbar@geo.haifa.ac.il (M. Inbar).

0377-0273/$ – see front matter © 2010 Elsevier B.V. All rights reserved.
doi:10.1016/j.jvolgeores.2010.07.013

morphological studies, together with remote sensing, tephrochronology and methods of absolute dating, are efficient tools for determining ages of cinder cones, their morphological evolution and spatial–time development of aerial volcanic fields all over the world and in extraterrestrial conditions.

The large Kamchatka volcanic field (Russian Far East), with probably the largest number of monogenetic cinder cones in the world, is an excellent case study for spatial and temporal classification. Many zones of monogenetic volcanism exist, with tens of cinder cones (such as the Tolbachinsky, Tolmachev and Sedanka fields), and fields of parasitic cones on the slopes of large volcanoes (such as Kliuchevskoy plateau). Cones are located all along the ~1000 km of the Kamchatka volcanic belt, at various elevations above sea level; they are of different types of pyroclastic components. In particular, they are located at various distances from large volcanic centers, that is, they are covered by soil-pyroclastic successions of different thickness, and this influences their morphometric features.

Kamchatka peninsula, like many other volcanic areas of the world, is blanketed by a soil-pyroclastic cover, representing the alteration of ashes of different volcanoes and buried soils (peat) or sandy loams. This cover is a few tens of centimeters thick in areas far from the active volcanoes and increases up to several meters at their source. The continuously accumulating soil/peat-pyroclastic successions in the areas under the Late-Pleistocene glaciation are usually of Holocene ages; older covers have been eroded by series of glaciations.

The Late Pleistocene and Holocene cinder cones are well preserved in Kamchatka while older forms (e.g. of Early–Middle Pleistocene age) are markedly eroded due to geomorphic processes, particularly during the last stage of the Pleistocene glaciation.

Unlike other large volcanic fields with hundreds of monogenetic cinder cones, such as the Michoacan-Guanajuato (Mexico), San Francisco (Arizona, USA), Andino-Cuyano (Mendoza, Argentina), Tenerife (Canary Islands, Spain) and Hawaii with a long list of published works (Scott and Trask, 1971; Porter, 1972; Bloomfield, 1975; Settle, 1979; Martin del Pozzo, 1982; Dohrenwend et al., 1986; Wolfe et al., 1987; Hooper, 1995; Inbar and Risso, 2001; Dóniz et al., 2008, among others), the Kamchatka cinder cone field enjoys few morphological studies (Syrin, 1968; Dirksen and Melekestsev, 1999); no detailed morphometric work at all has been published on this volcanic province.

The introduction of digital elevation models (DEM) as digital representation of surface topography has made precise quantitative estimation of cinder cone characteristics, possible. Parrot (2007) presented a method for accurate calculation of various geomorphic parameters from high-resolution DEMs (Chichinautzin Range Volcanic Field, Mexico) to simulate the evolution of a given shape and then to estimate the volume of material removed during erosion. Kervyn et al. (2008) performed a comparative analysis of the accuracy of DEMs provided by ASTER (Advanced Space-borne Thermal Emission and Reflection Radiometer) and SRTM (Shuttle Radar Topographic Mission), focusing on retrieval of quantitative morphometric data for moderate and small-sized volcanic features.

The aims of this study were: a. to examine the morphology and morphometric relationship among the monogenetic cones in the Kamchatka cinder cone field, with measuring to be done mostly in the field; and b. to analyze their relative ages as compared with absolute dates. This would allow a new interpretation of the sequence development of the volcanic field, as well as the rate of erosional processes in the climate of the Kamchatka Peninsula compared with volcanic fields in different climates in the world to examine the consistency of morphometric characteristics estimated from digital elevation models (DEM) of nine monogenetic cones within the Tolbachik volcanic field. Four “new” cinder cones were recently formed during the Great Fissure Tolbachik Eruption (GFTE) of 1975–1976 and five “old” cones were formed during the last 1700 years.

2. Physical background

Kamchatka forms the northern segment of the Kurile-Kamchatka island arch which is a part of Pacific “fire ring.” This peninsula extends for ca 1300 km, SW to NE between 51° and 62° N. Kamchatka and the adjacent Kurile Islands are the above-water part of a 2000-km asymmetrical range, separating the Sea of Okhotsk from the Pacific Ocean (Ponomareva et al., 2001), underwater part is 300–700 km wide; the maximum width of the landmass is 420 km. Main property of the last 100 million years of Kamchatka geological history is the continuous magmatic and volcanic activity proceeding at varying intensity over time. For most of the Cenozoic period an orogenic foldbelt was developed, and in the Pliocene–Pleistocene a volcanic arch developed with adequate volcanic processes and landforms.

The modern climate is very humid in most of the peninsula, with precipitation rate ranging from 2500 mm/year on the east coast to 500–800 mm/year in the central part of Kamchatka. Winters are cool and snowy and summers are wet and cloudy (Solomina et al., 2007).

The Tolbachik cinder cone field is one of the youngest volcanic landforms in Kamchatka, located in the SW part of the Kliuchevskaya volcanic group, which is the largest in Kamchatka (Fig. 1). The Tolbachik field is a huge, inclined lava plane, formed as a result of abundant eruptions of many cinder and lava cones and some fissure eruptions, with a total surface area of 875 km^2 and these volcanic centers are related to the 70-km long Tolbachik regional cinder cone zone. This zone has a NNE bearing (azimuth 20°–25°) in the south crossing the Plosky Tolbachik volcano, and changing direction to NE (azimuth 40°–45°) (Fig. 1).

3. Tolbachik — chronology of eruptions

The Tolbachik cinder cones erupted during the last ten kiloyears (ky) at 200–2500 m a.s.l. The lower time boundary estimation was based on the evidence that the moraine of the last Upper Pleistocene glaciation was covered by lava and pyroclastic deposits of the oldest cinder cones. The age-related cinder cone groups were subdivided based on tephrochronological studies together with extensive radiocarbon dating. The following cinder deposits of catastrophic volcanic eruptions were used as marker ash layers (Braitseva et al., 1993): Young Shiveluch, Ksudach, Khangar and Kizimen. As a result, six age-graded groups were defined:

(1) 10–7.5 ky
(2) 7.5–2 ky
(3) 2–1.5 ky
(4) 1.5–1 ky
(5) 1–0.3 ky
(6) Recent eruptions (1740, 1941 and 1975–1976)

The last, huge eruption of 1975–1976 was the youngest volcanic episode of the Tolbachik field activity during the Holocene; and there were ca 60 volcanic episodes during the last 10–11 ky. During the last 2 ky large cinder cones were formed, composed of magnesia basalts, like the northern cones of the GFTE. Cones formed earlier are far smaller in size and volume. Despite the short-term span of cinder cone existence (only 10–11 ky) their surface morphology (especially of the oldest cones) notably changed (Fig. 2).

4. The 1975–1976 eruption

The Great Tolbachik Fissure Eruption (1975–1976) is the youngest eruption of the Tolbachik cinder cone field, when cinder cones of various in dimension, morphology and chemical composition formed. The eruption started on June 28, 1975 from weak explosions from the Plosky Tolbachik summit crater. On July 6, the Northern cones started to form.

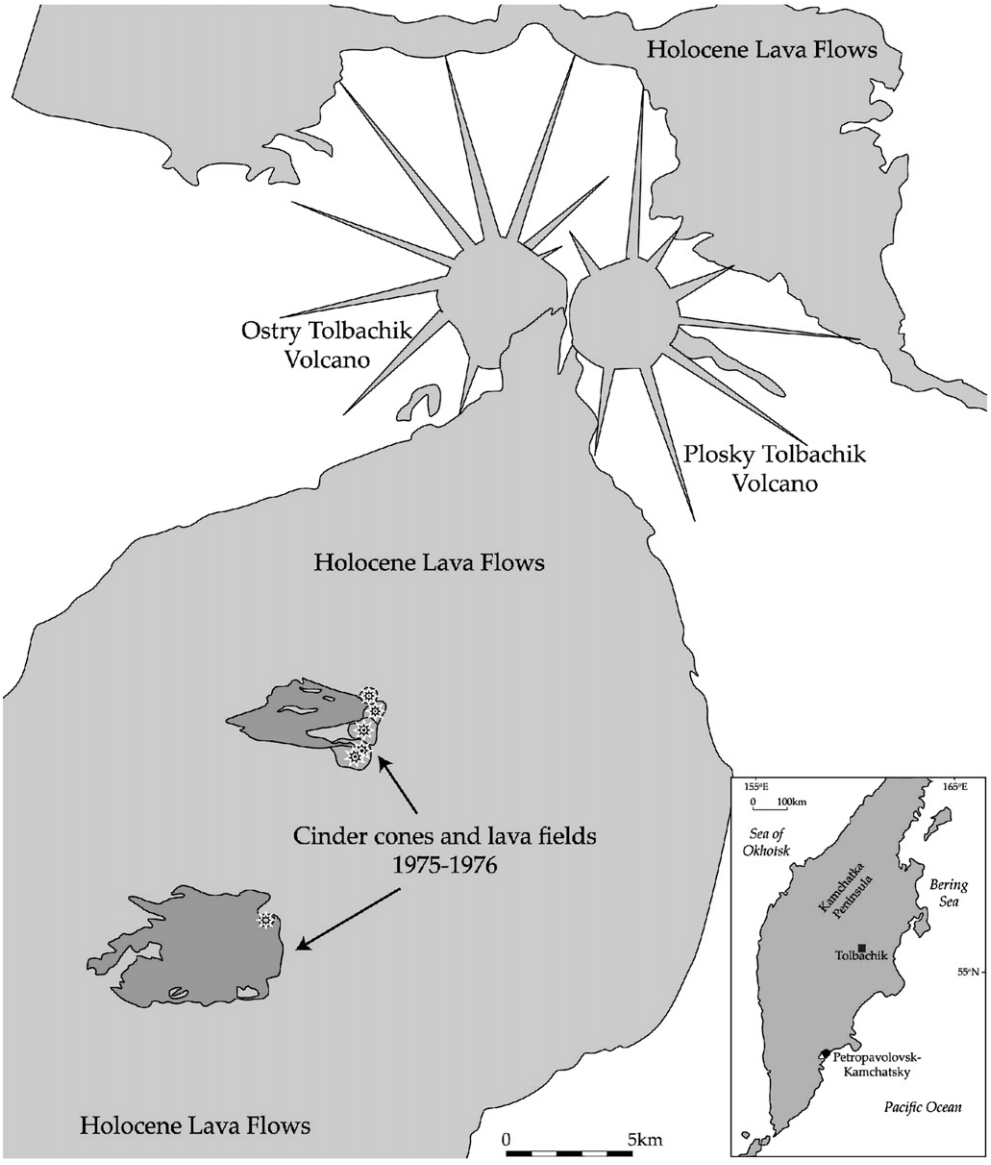

Fig. 1. Location map of the study area and overview of Kamchatka peninsula. Northern and Southern fissures of Great Fissure Tolbachik Eruption (GFTE) are depicted in dark grey on the grey background of Holocene lava flows.
Adapted from Fedotov and Masurenkov, 1991.

During the 72 days of Northern Fissure activity, three cinder cones formed, together with a lava field ($S = 8.86\ km^2$) with a lava cover 80 m thick (northern dark grey area in Fig. 1). At the end of August 1975 the parameters of the cinder cones were measured from aerial photo data: I — height 299 m and volume 0.133 km^3; II — 278 m height and volume 0.099 km^3; and III — 108 m height and volume

Fig. 2. View of Kamenistaya old cone (left) and cone Yuzhniy (right) erupted in 1976. Slope values are 23° and 31° respectively.

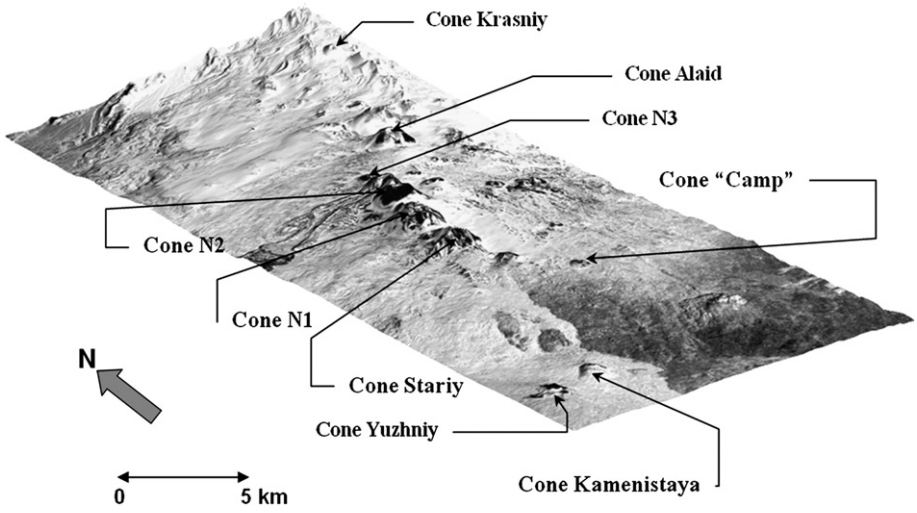

Fig. 3. Perspective view of the study area presented by ASTER DEM.

0.022 km^3 (Dvigalo et al., 1980). Their total volume was estimated at 0.254 km^3 and the weight of composing rocks at 0.38×10^9 tons ($\rho=1.5$ g/cm^3). The primary slope angle of the cones was 30°–35°. Only 28% of total volume and 34% of total weight of erupted pyroclastic rocks (0.921 km^3 and 1.117×10^9 tons) formed the cinder cones. The respective mean rates of pyroclastic outflow were 178 m^3/s and 214 tons/s. The total volume of lavas was 0.223 km^3 and the weight was 0.49×10^9 tons ($\rho=2.2$ g/cm^3).

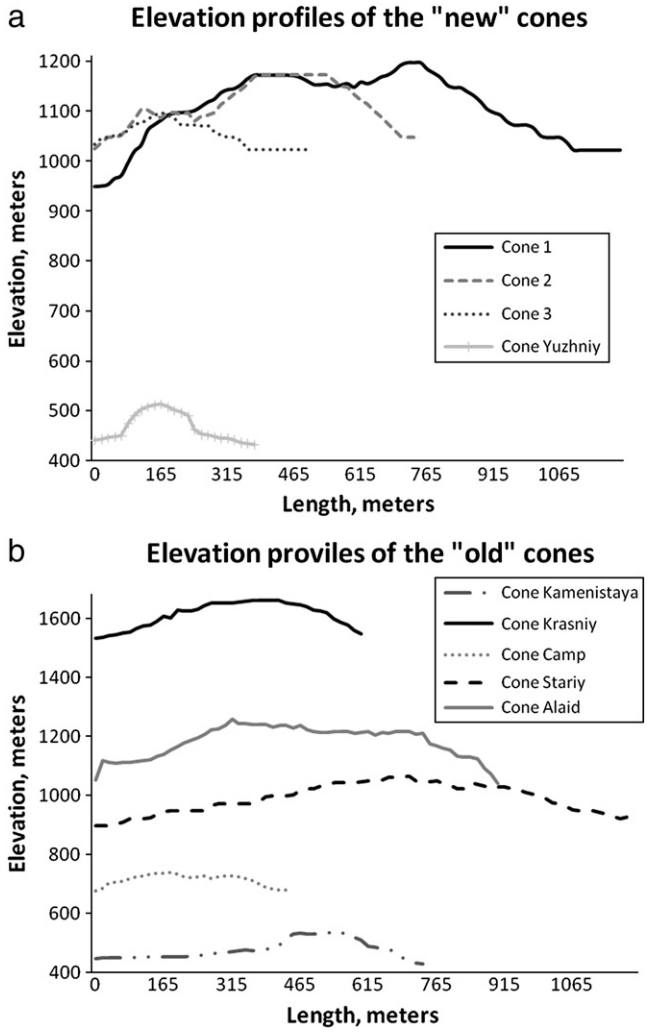

Fig. 4. Field measured elevation profiles of recent (a) and old studied cinder cones (b). Note that height is given as absolute elevation above sea level ground (photo August 2007).

The lavas and pyroclastic rocks of the Northern Fissure had similar chemical composition and are mostly magnesia medium alkaline basalts (49.54–49.75% of SiO_2, 9.84–10.21% MgO, 2.38–2.44% Na_2O, 0.97–1.02% K^2O) according to 35 samples analyzed (Braitseva et al, 1997).

Remarkably, the previous eruption which took place in 1941 had similar eruption dynamic, parameters (i.e. rate of pyroclasts and lava volume) and chemical composition to those of the Northern Fissure eruption. We can reasonably assume that the above peculiarities of magnesia basalt cinder cone formation and the dynamic parameters of their eruption had been characteristic for the older cinder cones which started forming at the Tolbachik field ca 2000 BP (Braitseva et al., 1997).

The Southern cone appeared 10 km SW of Cone I of the Northern Fissure at 380 m a.s.l. and erupted ca 450 days (6 times more than the Northern Fissure). Its activity was quieter version of Strombolian-type eruption. A single relatively small cone formed: its maximum height was 165 m, rock weight — 0.024×10^9 tons ($\rho=1.5$ g/cm^3), the volume — 0.016 km^3 (together with cone fragments dragged down by lava flows). The relative height of the cone (after the eruption ceased) was 85–120 m (its base was buried under lava flows 80 m thick). The main result of the Southern cone eruption was the formation of a huge lava cover ($S=35.87$ km^2, $V=0.968$ km^3 and weight $=2.14\times10^9$ tons).

The moderate and weak explosive activity of the Southern cone caused most of pyroclastics (53%) to accumulate on the cone itself: 47% was blown away by the wind. The lavas and pyroclastics of the South cone consist of subalkalic, aluminous basalts (50.67–50.85% SiO_2, 4.58–4.98% MgO, 3.52–3.62% Na_2O, 1.85–2.11% K_2O, 133 samples analyzed) (Flerov et al., 1984).

5. Methodology

5.1. Field measurements

In our fieldwork in August 2007 on the Tolbachik cinder cone field (GTFE area) we studied the morphometry of the nine cinder cones located along the main sub–meridian fault (Fig. 3). The cones lie at various altitudes (350–1500 m a.s.l.), and the distance between the outermost Yuzhniy cone on the south and the Krasny cone on the north is 20 km (Fig. 3).

Fig. 5. Trees burnt during the 1975 eruption. Grass and moss vegetation developed on ground (photo August 2007).

The elevation measurements were obtained as WGS84 ellipsoid heights by a Fujitsu–Siemens Pocket LOOX N560 (Sirf III GPS chipset). This handheld GPS device provides a horizontal accuracy of about 3 m and its error in elevation can be as high as 7–9 m. In total we collected GPS data at 85 locations within the study area including 73 measurements of randomly oriented elevation profiles of the nine cinder cones. We thus obtained a series of elevation profiles based on 8–10 observation points each profile (Fig. 4).

The ground control points (GCP) were corrected to geoid heights (EGM96) and used in DEM generation, employing the DEM Extraction Module (ENVI™ 4.6). The GPS measurements were also used to evaluate the accuracy of the DEMs generated from ASTER remotely sensed data.

The recent cones are surrounded by a scoria covered plain where vegetation cover is about 10% and most of it are mosses. No vascular plants were found in the new cones. Trees in the affected area by the eruption were completely burned (Fig. 5) and in the cones area no burnt tree trunks remained. Most of the new cinder cones surrounding area is covered by tephra and lava, on the base of the cones megablocks were found about one meter diameter (Figs. 6 and 7).

Depth of craters in the recent cones is about 50 m (Fig. 6) and they are unbreached in all the cones, except Cone N2. In all cones slopes are steep and built of about 50% of lapilli and scoria material of the surface slope. They are not dissected except for trails of big volcanic bombs. In Cone N2 “bocca lava” was found close to the crater that breached the cone flank. The old cones are eroded by breaching with broad tails in their base, as evidence of mass wasting processes.

5.2. Morphometric measurements

Morphometric measurements from the DEM derived from ASTER optical imagery with 30 m of spatial resolution were taken, and these were compared with measurements done on 1:25,000 topographic maps. For every studied cinder cone we calculated the main morphometric parameters from these two elevation data sources. They include cone height (h), steepest cone slope, major-axis diameter (d_{mj}), short axis diameter (d_{mi}), and height–width ratio (h/W), where h is the relative height and $W = (d_{mj} + d_{mi})/2$. We took field GPS measurements (plane coordinates and elevation) of 40 locations to provide geodetic reference for DEM processing and also to validate the calculated DEMs at additional 45 locations (Fig. 8).

5.2.1. Topographic maps

Cone height (h), cone width (W), h/W ratio and slope angle calculated from topographic maps are the main morphometric parameters used for determining the rate of cone degradation as a function of its exposure to erosion (Wood, 1980a, b). The standard definition of these parameters is based on measurements derived from topographic maps. In Hooper and Sheridan (1998) cone width is calculated as the average of the maximum and minimum basal diameters for each cone and cone height is defined as the difference between average basal elevation and maximum crater rim or summit elevation. The methodology adopted to measure the morphometric parameters over topographic maps is similar to that introduced by Wood (1980a) and summarized by Hooper (1995). Cone basal diameter was measured from topographic maps and calculated as the mean of the maximum and minimum basal diameters of each cone. Cone height was measured as the difference between the highest and the average basal elevation.

The mapping of erupted material from four cinder cones was carried out already during GFTE whereas the entire Tolbachik volcanic field was topographically surveyed at a scale of 1:25,000 in 1976–1980. In this study we used topographic maps of the Tolbachik volcano field on a scale of 1:25,000 were used for calculation of morphometric parameters and for providing comparable basis with DEM-based morphometric measurements (Fig. 9a and b).

5.2.2. ASTER DEM

The present research uses remotely sensed imagery of ASTER (Advance Space-borne Thermal Emission and Reflection Radiometer). This is cloudless (March 2004) Level 1A ASTER image products (Reconstructed Unprocessed Instrument Data V003) and orthorectified Level 3 images. The visible near infra-red sensor of Level 1A ASTER products (with 15 m of spatial resolution) includes nadir-

Fig. 6. Cone N3, erupted 1975 (August 2007).

looking (VNIR3N) and backward-looking (VNIR3B) scenes of the same point on the surface. This creates the effect of automatic stereo correlation which is used for DEM generation with spatial resolution of 15 m. Generally, the root mean square error (RMSE) in ASTER DEM elevations ranges from ±7 m to ±15 m, depending on availability and quality of GCPs (known ground control points) and image quality (Hirano et al., 2003). In vegetationless areas ASTER digital elevation models are expected to approach a better vertical accuracy (about 10 m) (Goncalves and Oliveira, 2004; Hirano et al., 2003) which allows morphometric measurements with accuracy similar to medium-scale topographic maps (1:50,000).

The procedure for deriving DEM from ASTER data began with a definition of the study area (Tolbachik volcano field) cropped from the entire ASTER imagery (60*60 km), for VNIR3N and VNIR3B bands. The next step was orthorectification of these two bands by rational polynomial coefficients (RPC) of sensor geometry, accordingly to image metadata and ASTER product documentation. Then DEM was generated by means of the ENVI 4.3 DEM extraction wizard using the

Fig. 7. Northern Fissure cinder cones, lava and tephra covered surrounding area, erupted 1975, on the background of Tolbachik volcano (August 2007).

Fig. 8. The view of the crater of Cone N1.

orthorectified VNIR3N band as a left stereo image and the orthorectified VNIR3B band as a right one. In this process RPC are used to generate tie points and to calculate the stereo image pair relationship. The availability and accuracy of ground control points that can be located precisely on ASTER stereo pairs determine the accuracy of the absolute orientation. Accordingly, we used field GPS measurements of 40 locations covering nine cinder cones as ground control points to tie the horizontal and vertical reference systems to UTM geodetic coordinates. As a result absolute horizontal and vertical orientation was achieved. The final DEM was generated at spatial resolution of 30 m. Holes in the generated DEM were filled by automated interpolation, and then smoothed by 3×3 low-pass filter to reduce the effect of possible artifacts caused by enhanced recognition of topographic features. For visualization of the obtained DEM (Fig. 10), isolines were generated and then each studied cinder cone was topographically separated from the surroundings, accordingly to basal isoline.

Definition of the base of a cinder cone allows for the separation of each cinder cone from its topographic vicinity. In our study the base of the cinder cone was allocated by the lowest elevation isoline with an average of slope pixels more than 5°. The basal plane elevation was estimated as the average elevation value of all DEM pixels located along the basal outline. Then we calculated the slope of the cinder cone as the average of pixel slope values situated along the steepest profile with the greatest elevation difference (cone height, h) between the highest cone point and the basal outline on the shortest horizontal distance. The basal isoline was fitted to an ellipse shape by means of an ad-hoc developed IDL program, to facilitate the width measurements. Then the cone width (W) was calculated as the average of the maximum and minimum axes of this ellipse.

The slope is usually defined as a plane tangent to a topographic surface of the DEM at a given pixel (Burrough, 1986). To derive the slope information from the ASTER DEM, the topographic modeling procedure of ENVI 4.3 was performed to produce slope values in degrees for every pixel in the DEM. Thus, the steepest slope of the cinder cone was calculated as an average of pixel slope values for the profile with the highest run/rise ratio (largest elevation difference between the cone's highest point and the basal isoline on the shortest horizontal distance).

6. Results

Morphometric parameters of nine cinder cones on the Tolbachik volcano field were calculated from ASTER DEM and topographic maps (Table 1). All these cinder cones are higher than 50 m and could be easily identified on the landscape by visual examination of a three-dimensional view of DEM (Fig. 11). For all observed cinder cones the volume values (in km^3) were derived from ASTER DEM.

The studied cinder cones were divided into two groups, according to age of eruption. The youthful cones formed during the last Tolbachik eruption (1975–1976) and the older ones during last 1500–1700 years which were dated by tephrochronology and ^{14}C. The field GPS measurements of these cones show the cross-section elevation profiles (Fig. 4). Some morphologically complex cones in ASTER DEM (with fewer GCPs) were subject to error, due to excessive interpolation (e.g. Cone N3) or because of blunder artifacts (e.g. Krasniy cone). Fig. 11 shows a general view of the observed cinder cones (accordingly to ASTER DEM) which vary in size, morphology complexity and the volume of pyroclastic material (Table 1).

The cones height value derived from the ASTER DEM and from the topographic maps are similar, ranging from ~50 to ~240 m. The main morphometric parameters of slope and height/base ratio according to ASTER DEM (30 m of grid cell) prove significant correlation with old and new cone age groups (Table 1). In all studied cones of ASTER DEM the highest slope values correspond to the recent cones (Table 1). The average slope for the recent cones group is 31.9° (ASTER DEM) and 31.7° (MAP); the "old" cone group shows considerably smaller average slope values: 26.3° and 27.1°, respectively. Association of high values with modern cones is also evident in h/W ratio (except Cone N3 and Cone Krasniy). Average values of height–base ratio are: 0.22 (ASTER) and 0.21 (maps) for recent cones; 0.17 (ASTER) and 0.16 (MAP) for older cones. A possible reason for discrepancy of h/W ratio of Cone N3 and Cone Krasniy might be the comparatively complex morphology of these constructions, which have an effect on the measurements. By definition

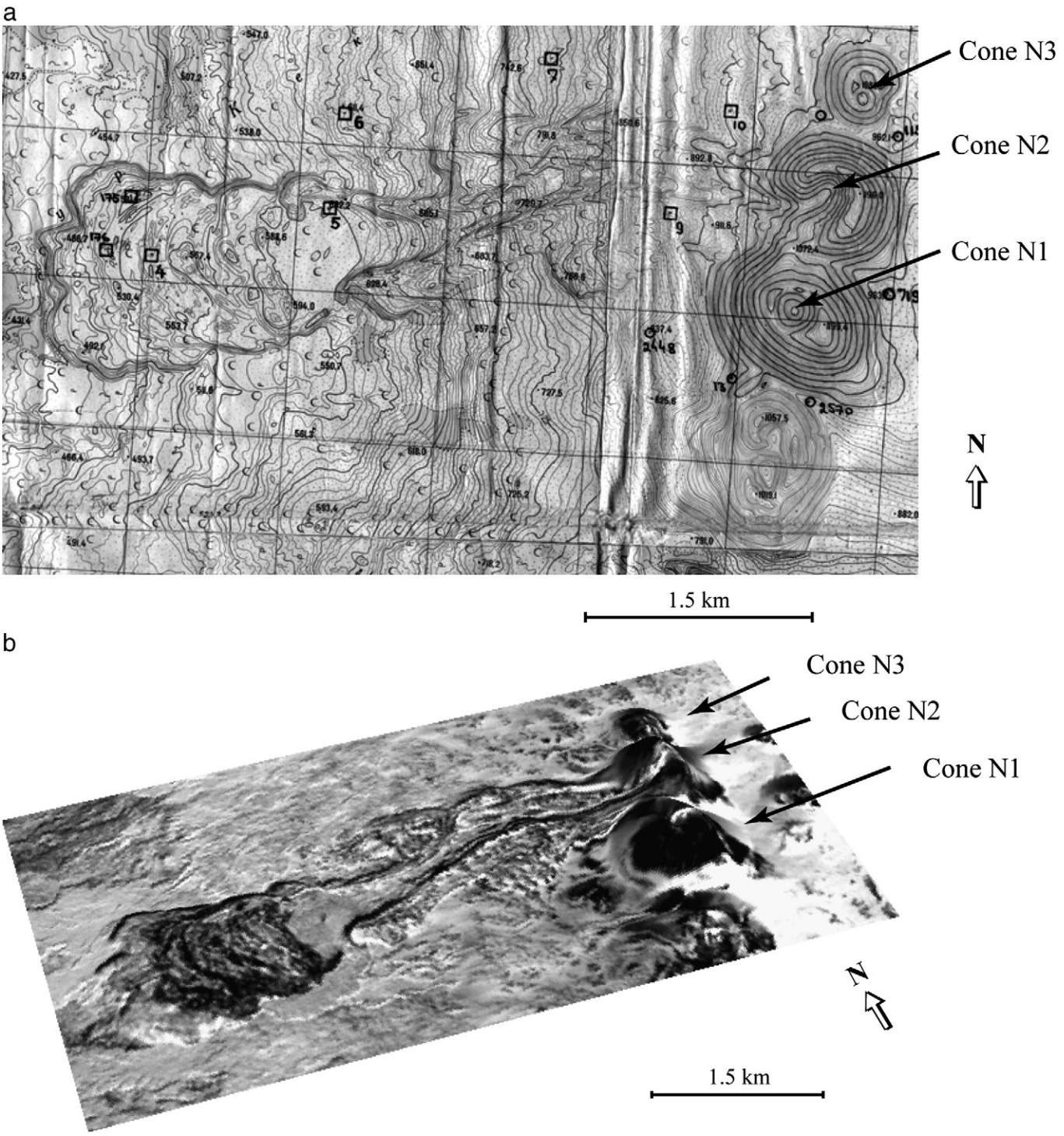

Fig. 9. (a) Three GFTE cones of the Northern fissure on the 1:25,000 topographic map; (b) the perspective view of three GFTE cones of the Northern fissure in ASTER DEM.

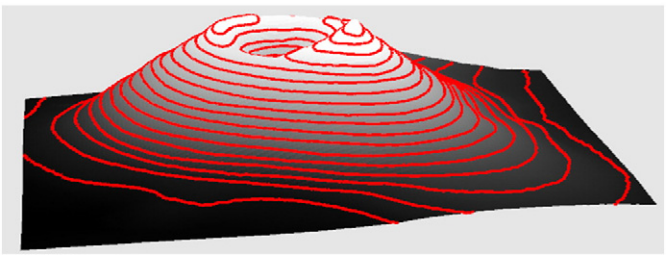

Fig. 10. The DEM (Cone N1) with over draped isolines.

ASTER data have lesser spatial and height accuracy than the topography map; nevertheless in our case similar morphometric characteristic were obtained. This finding also verifies the reliability of DEM-based volume calculations. In the “old” cone group the cones of smaller volume have been associated with smaller h/W ratio. The h/W ratio reflects the cone's degradation rate, decreasing with age, as material is removed from the crest to the cone base. For recent GFTE cones the obtained h/W values were above 0.18 and actually reached 0.26 for Cone N2 according to ASTER DEM measurements (0.24 according to the topographic map). The average h/W ratio of cinder cones dated as several thousands of years was about 0.15 for DEM and maps measurements.

Table 1
Morphometric parameters of nine cinder cones of Tolbachik volcano field measured from ASTER DEM and topography maps.

			Volume, km^3	Cone height (h), m		Cone slope (s), degrees		Mean basal diameter (D), m		Height–base ratio (h/D)	
				ASTER	MAP	ASTER	MAP	ASTER	MAP	ASTER	MAP
Recent cones	1	Cone N1	0.135	239	228	32.4	32.0	1125	1050	0.21	0.22
	2	Cone N2	0.097	205	211	32.7	31.8	800	870	0.26	0.24
	3	Cone N3	0.017	97	95	31.5	32.0	533	525	0.18	0.18
	4	Cone Yuzhniy	0.016	117	113	31.2	31.0	550	550	0.21	0.21
"Old" Cones	5	Cone Krasniy	0.086	202	138	29.1	29.5	810	700	0.25	0.20
	6	Cone Alaid	0.118	226	230	28.8	32.0	1409	1325	0.16	0.17
	7	Cone "Stariy"	0.120	96	107	26.9	27.7	901	825	0.12	0.13
	8	Cone "Camp"	0.009	56	70	25.2	23.5	425	500	0.13	0.14
	9	Cone Kamenistaya	0.017	107	109	21.6	23.0	603	650	0.18	0.17

Despite the appearance of small-scale artifacts (caused by stereo pair matching) the concentration of field GCPs over the studied cones led to their realistic representation in ASTER DEM (Fig. 11). The spatial accuracy of ASTER DEM has been evaluated by comparison of DEM value to field ground control points (Table 2). The evaluation of horizontal and vertical root mean square error (RMSE) of each cinder cone has demonstrated acceptable level of accuracy, typical for DEMs derived from ASTER data. In all cinder cones vertical errors were significantly higher than horizontal, especially among old cones where vertical error often appeared about three times greater than horizontal.

7. Discussion

The evolution of the Tolbachik volcanic landscape, 31 years after cessation of the volcanic activity, with a number of recent monogenetic cinder cones offers the opportunity to learn about the development of the landscape, a central issue in geomorphologic

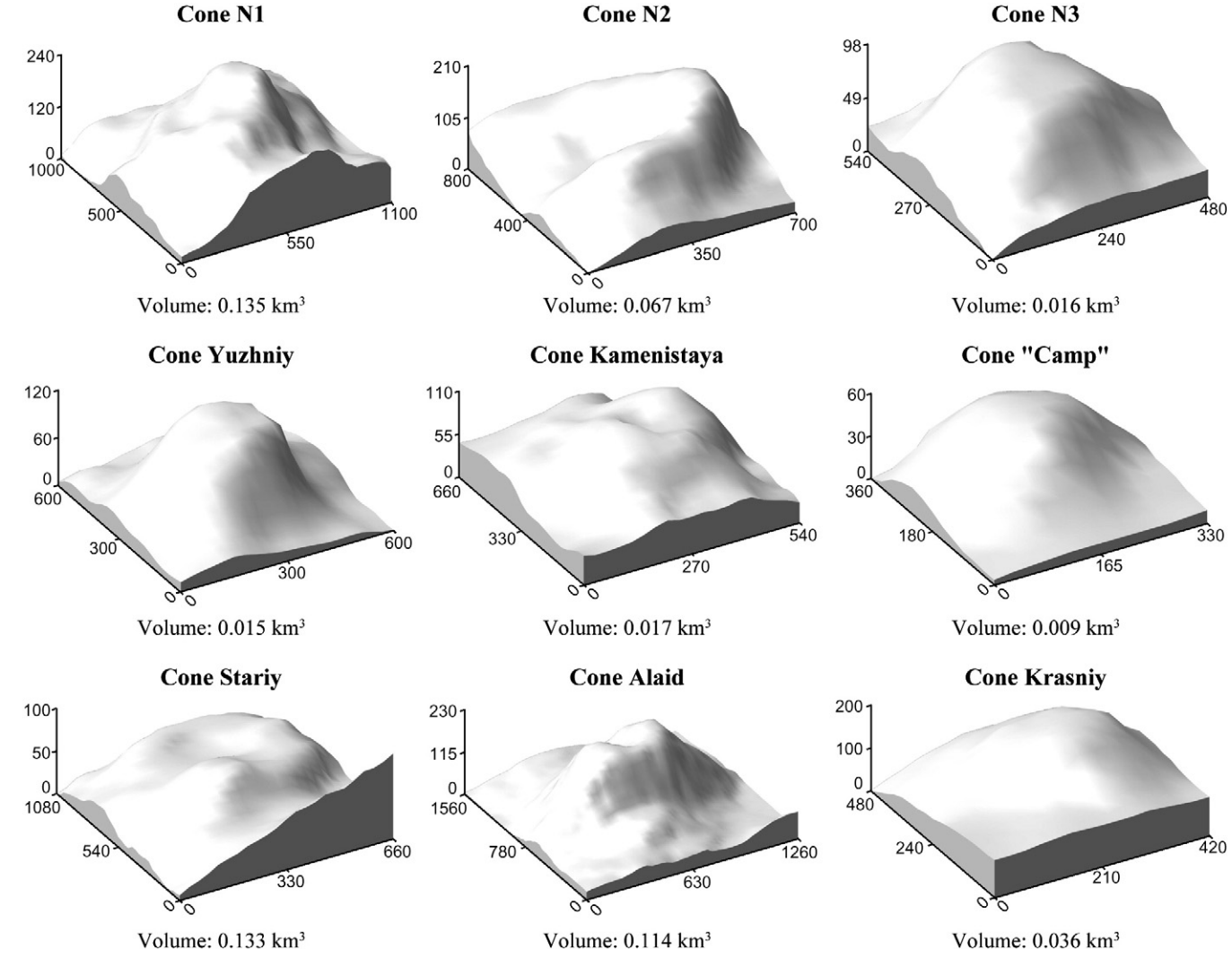

Fig. 11. Digital elevation models of nine cinder cones studied: a — Cone N1; b — Cone N2; c — Cone N3; d — Yuzniy; e — Kamenistaya; f — Cone "Camp"; g — Cone Stariy; h — Cone Alaid and i — Cone Krasniy. Note the visual difference in the shape of new (a–d) and old cones (e–i).

Table 2
Distribution of horizontal and vertical RMS errors of the ASTER DEM for the nine cinder cones studied.

			RMSE Vertical, m	RMSE Horizontal, m
Recent cones	1	Cone N1	9.9	14.6
	2	Cone N2	9.6	14.8
	3	Cone N3	8.4	13.1
	4	Cone Yuzhniy	8.3	12.2
"Old" Cones	5	Cone Krasniy	15.1	23.3
	6	Cone Alaid	10.6	16.9
	7	Cone "Stariy"	9.0	12.9
	8	Cone "Camp"	9.3	13.7
	9	Cone Kamenistaya	4.1	6.1

studies. The h/D ratio values for the recent cones as high as 0.21 (ASTER DEM) or 0.27 (MAP), are consistent with the published data for several areas in the world in different climatic conditions (Inbar and Risso, 2001). There is a clear relationship between slope and h/W ratio, according to Woods (1980b) predicted curve (Fig. 12) The Tolbachik cones have high slope values like the Paricutin, Navidad and other new cones (Moreno and Gardeweg, 1989; Inbar et al., 1994).

This paper assessed the capability of remotely sensed ASTER DEM for morphometric measurements of cinder cones on the example of the Tolbachik volcanic field in Kamchatka. The morphometric parameters of cone slope, height and width were calculated from the remotely sensed DEMs and compared with the morphometric parameters measured from the topographic map (Table 1).

Morphometric parameters were calculated for the nine cinder cones studied, divided into two age groups of recent and older cones. ASTER DEM and topographic map were compared to assess different methods on morphometric measurements of height, width, h/W ratio and slope. The morphometric parameters calculated from ASTER DEM and topographic map are numerically different from each other but well correlated with age groups of cinder cones. For example, calculated from both ASTER DEM and topographic map, all the four recent cones have the highest slope values; the two cones with the highest slopes (Cones N1 and N2) correlate with the highest values of h/W ratio (Table 1).

The comparison of morphometric parameters calculated from ASTER DEM and topographic map clearly supports the concept of relative morphometric dating as the most recent cinder cones are always associated with the highest slopes and h/W ratio (Table 1). However, in DEM spatial resolution controls the ability to represent local topography of cinder cones by interpolation of elevation data points in the vicinity of breaks in slope. From other hand, the morphometric measurements from topographic maps might be affected by subjective decisions of the analyst. Thus, the straightforward numerical comparison of morphometric values calculated from DEM and topographic maps might be erroneous. In such a case, calculated morphometric parameters might be affected by smoother representation of the surface in coarse-resolution DEMs. Similarly, the comparison of DEMs of different spatial resolution when younger cinder cones depicted on a coarse-resolution DEM might result in the similar morphometric values as older cones calculated from a high-resolution DEM. For correct morphometric dating of the cinder cones series we suggest the comparison of morphometric parameters systematically calculated from the one source of elevation data.

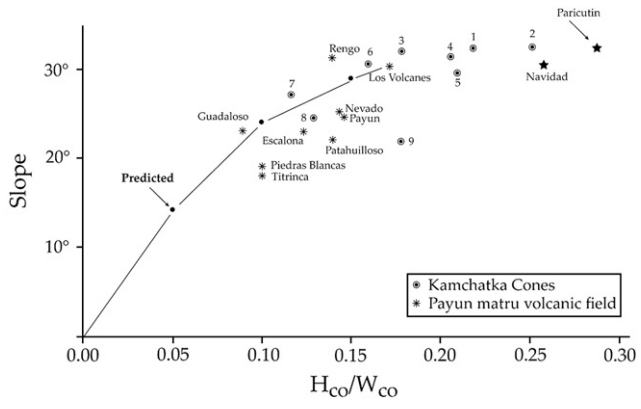

Fig. 12. Cone slope values and Hco/Wco ratio values for cinder cones in the Payun Matru Volcanic Field, Navidad cone and Tolbachik cones. Predicted curve is from weathering and mast wasting model by Wood (1980b). Note that numeration of Kamchatka cones conforms their order in Tables 1 and 2.

The accuracy of ASTER DEM has demonstrated typical spatial error for DEMs derived from ASTER data (Table 2) which we found suitable for morphometric measurements on small-scale pyroclastic constructions like cinder cones.

The influence of climate is reflected in the highest rates of erosion of the area, due to the harsh weather conditions. The slope angle decreases from an initial value of 31°–34° for the 1975 cones to 25°–29° for the cones 1500–2000 years BP. The Paricutín cone in Mexico erupted in 1943 had an initial slope of 31° to 33° (Segerstrom, 1950) declining slightly to 32° and 31°, 45 years later (Inbar et al., 1994). There is a rapid decline of the slope values in the first stage of erosion. Recent cones on Mt Etna show a similar slope decrease of 10 degrees in only 450 years (Wood, 1980b). Cone evolution shows erosional rounding of rim and deposition at base, in accordance with linearly slope-dependent transport models (Pelletier and Cline, 2007).

The measured morphometric parameters of the recent Tolbachik cinder cones are important for determining erosion rates, as the measured erosion values for the Paricutin cone after the 1943 eruption (Segerstrom, 1950) and the Navidad cone erupted in December 1988 in Chile (Moreno and Gardeweg, 1989). A comparison with the cinder cones older by several millennia in the area shows that the climatic conditions and the slow development of vegetation cover determine high rates of erosion and rapid change in morphometric values. Variability in morphometric values of the recent cinder cones is due to their lithological coarse composition.

Peaks of erosion occurred probably in the first stage of 1 or 2 years after the eruption, with the stripping of the fine ash material, as recorded in several volcanic areas of the world (Swanson et al., 1983). Accelerated peaks of erosion were also measured after forest fires in non vegetated areas (Inbar et al., 1998).

The morphometric parameters of the recent Tolbachik cinder cones serve as a valuable benchmark data for determining erosion rates and future research on the geomorphological evolution of volcanic landscape.

The erosional processes in the climatic conditions of the Kamchatka peninsula are more intensive than the published values for other cinder cones in volcanic fields (e.g. the subtropical climate of the Mexican Volcanic field (Hooper, 1995), the semiarid climate of Payun Matru Volcanic Field (Inbar and Risso, 2001), or the Mediterranean climate of the Golan plateau (Inbar et al., 2008) showing measurable morphological changes in the range of thousands of years.

Acknowledgments

The research was supported by the Ministry of Science of Israel grant 3-3572 and the Russian Foundation for Basic Research. The authors are grateful to the Institute of Volcanology and Seismology in Petropavlosk-Kamchatsky, Russia for logistic support of the study. We thank the two reviewers for their constructive comments on the manuscript.

References

Bloomfield, K., 1975. A late-Quaternary monogenetic volcanic field in central Mexico. Geologischen Rundschau 64, 476–497.

Braitseva, O.A., Melekestsev, I.V., Litasova, S.N., Sulerzhitsky, L.D., Ponomareva, V.V., 1993. Radiocarbon dating and tephrochronology in Kamchatka. Radiocarbon 35 (3), 463–477.
Braitseva, O.A., Ponomareva, V.V., Sulerzhitsky, L.D., Melekestsev, I.V., Bailey, J., 1997. Holocene key-marker tephra layers in Kamchatka, Russia. Quaternary Research 47, 125–139.
Burrough, P.A., 1986. Principles of Geographical Information Systems for Land Resources Assessment. Clarendon Press, Oxford. pp. 147–166.
Dirksen, O.V., Melekestsev, I.V., 2000. Chronology, evolution and morphology of plateau eruptive centers in Avacha River Area, Kamchatka. Vulkanologia i Seismologia 21, 617.
Dohrenwend, J.C., Wells, S.G., Turrin, B.D., 1986. Degradation of Quaternary cinder cones in the Cima volcanic field, Mojave Desert, California. Geological Society of America Bulletin 97, 421–427.
Dóniz, J., Romero, C., Coello, E., Guillén, C., Sánchez, N., García-Cacho, L., García, A., 2008. Morphological and statistical characterization of recent mafic volcanism on Tenerife (Canary Islands, Spain). Journal of Volcanology and Geothermal Research 173, 185–195.
Dvigalo, V.N., Selezniov, B.V., Magus'kin, M.A., 1980. New results of aerial photo analysis of the Great Fissure Tolbachik Eruption. Volcanology and Seismology 3, 90–93.
Fedotov, S.A., Masurenkov, Y.P., 1991. Active Volcanoes of Kamchatka, vol. 1. Nauka Publishers, Moscow, p. 21.
Flerov, G.B., Andreev, V.N., Budnikov, V.A., Tsurupa, A.I., 1984. Petrology of eruptive products. Great Tolbachik fissure eruption. Kamchatka, 1975–1976. Nauka, Moscow, pp. 223–284.
Goncalves, J.A., Oliveira, A.M., 2004. Accuracy Analysis of DEMS derived from ASTER Imagery. International Archives of Photogrammetry and Remote Sensing 35, 168–172.
Hasenaka, T., Carmichael, I., 1985. The cinder cones of Michoacán-Guanajuato, central Mexico: their age, volume, distribution and magma discharge rate. Journal of Volcanology and Geothermal Research 25, 104–124.
Hirano, A., Welch, R., Lang, H., 2003. Mapping from ASTER stereo image data: DEM validation and accuracy assessment. ISPRS Journal of Photogrammetry and Remote Sensing 57, 356–370.
Hooper, D.M., 1995. Computer-simulation models of scoria cone degradation in the Colima and Michoacan-Guanajuato volcanic fields, Mexico. Geofísica Internacional 34, 321–340.
Hooper, D.M., Sheridan, M.F., 1998. Computer-simulation models of scoria cone degradation. Journal of Volcanology and Geothermal Research 83, 241–287.
Inbar, M., Risso, C., 2001. A morphological and morphometric analysis of a high density cinder cone volcanic field — Payun Matru, south-central Andes, Argentina. Zeitschrift für Geomorphologie 45, 321–343.
Inbar, M., Lugo Hubp, J., Villers Ruiz, L., 1994. The geomorphological evolution of the Paricutin cone and lava flows, Mexico, 1943–1990. Geomorphology 57–76.
Inbar, M., Tamir, M., Wittenberg, L., 1998. Runoff and erosion processes after a forest fire in Mt. Carmel, a Mediterranean area. Geomorphology 24, 17–34.
Inbar, M., Gilichinsky, M., Melekestsev, I., Melnikov, D., 2008. A Morphological and Morphometric Study of Cinder Cones in Kamchatka and Golan Heights. Proceedings Israel Geological Annual Meeting, Nazareth, Israel, p. 44.
Kervyn, M., Ernst, G.G.J., Goossens, R., Jacobs, P., 2008. Mapping volcano topography with remote sensing: ASTER vs. SRTM. International Journal of Remote Sensing 29 (22), 6515–6538.
Martin del Pozzo, A.L., 1982. Monogenetic vulcanism in Sierra Chichinautzin, Mexico. Bulletin of Volcanology 45, 9–24.
Moreno, H., Gardeweg, M.C., 1989. La erupcion reciente en el complejo volcanico Lonquimay (Diciembre 1988), Andes del Sur. Revista Geologica de Chile 16,1, 93–117.
Parrot, J.F., 2007. Tri-dimensional parameterization: an automated treatment to study the evolution of volcanic cones. Geomorphologie 3, 247–258.
Pelletier, J.D., Cline, M.L., 2007. Nonlinear slope-dependent sediment transport in cinder cone evolution. Geology 35 (12), 1067–1070.
Ponomareva, V.V., Sulerzhitsky, L.D., Dirksen, O.V., Zaretskaya, N.E., 2001. Holocene paleosols as records of intervals of volcanic quiescence in the Kuril Lake region, South Kamchatka. Tephras, Chronology and Archeology. CDERAD Press, pp. 91–100.
Porter, S.C., 1972. Distribution, morphology and size frequency of cinder cones on Mauna Kea volcano, Hawaii. Geological Society of America Bulletin 83, 3607–3612.
Scott, D.H., Trask, N.J., 1971. Geology of the Luna Crater volcanic field, Nye County, Nevada. USGS Prof. Paper, 599-I. 22 pp.
Segerstrom, K., 1950. Erosion studies at Paricutin, state of Michoacan, Mexico. USGS Bull. 965-A 164 pp.
Settle, M., 1979. The structure and emplacement of cinder cone fields. American Journal of Science 279, 1089–1107.
Solomina, O., Wiles, G., Shiraiwa, T., D'Arrigo, R., 2007. Multiproxy records of climate variability for Kamchatka for the past 400 years. Climate of the Past 3, 119–128.
Swanson, F.J., Collins, B., Dunne, T., Wicherski, B.P., 1983. Erosion of tephra from hillslopes near Mount St. Helens and other volcanoes. Symp. on Erosion Control in Volcanic Areas, Seattle, July 1982. Public Works Research Institute, Ibaraki, Japan, pp. 183–221.
Syrin, A.N., 1968. Regional and Local Volcanism Relationship. Nauka, Moscow. 149 pp. (in Russian).
Thouret, J.C., 1999. Volcanic geomorphology — an overview. Earth Sciences Reviews 47, 95–131.
Wolfe, E.W., Ulrich, G.E., Newhall, C.G., 1987. Geologic Map of the Northwest Part of the San Francisco Volcanic Field, North-central Arizona. USGS Misc. Field Stud. Map, MF 1957.
Wood, C.A., 1980a. Morphometric evolution of cinder cones. Journal of Volcanology and Geothermal Research 7, 387–413.
Wood, C.A., 1980b. Morphometric analysis of cinder cone degradation. Journal of Volcanology and Geothermal Research 8, 137–160.